Turbulent pattern formation and diffusion in the early-time dynamics in relativistic heavy-ion collisions

Kenji Fukushima
Department of Physics, Keio University, Kanagawa 223-8522, Japan
(Received 17 July 2013; revised manuscript received 26 January 2014; published 18 February 2014)

We propose a picture of turbulent pattern formation in the relativistic heavy-ion collision, which follows an efficient process to break color strings and dispose energy in the whole phase space. We perform numerical simulations using the SU(2) pure Yang–Mills theory in a nonexpanding box to observe a dynamical phenomenon in the transverse plane akin to the domain growth in time-dependent spin systems.

DOI: 10.1103/PhysRevC.89.024907 PACS number(s): 25.75.−q, 05.45.Pq, 12.38.Gc

I. INTRODUCTION

Relativistic heavy-ion collision experiments at the BNL Relativistic Heavy Ion Collider (RHIC) and at the CERN Large Hadron Collider (LHC) have successfully created a quark-gluon plasma and probed into its detailed properties; among the milestones in quark-gluon-plasma research, the recognition of the so-called *perfect fluidity*, i.e., the smallness of the ratio of the shear viscosity to the entropy density was the most influential, which has triggered interdisciplinary discussions in many fields including nuclear physics and superstring theories.

Thanks to the tremendous developments of the lattice simulation of quantum chromodynamics (QCD) [1] and the (dissipative) hydrodynamic model [2], we have reached a reasonable understanding of the static properties of high-T QCD matter and the subsequent dynamical evolution. We are, however, still far from establishing a firm theoretical framework for the prethermalization stage. Generally speaking, the thermalization process out of equilibrium is a ubiquitous but complicated problem, and theoretical research mostly relies on numerical methods.

Luckily, in the case of relativistic heavy-ion collisions at sufficiently high energy, the very early-time dynamics on the time scale of the order of $\tau \sim Q_s \lesssim 0.1\ \mathrm{fm}/c$ can be expressed in terms of coherent gluon fields, where Q_s is the saturation momentum [3]. The initial state characterized by Q_s is sometimes referred to as the "glasma" initial condition [4]. In this glasma picture, most important is the presence of boost-invariant longitudinal chromo-electric and chromo-magnetic fields, $\mathcal{E}^\eta$ and $\mathcal{B}^\eta$, the intensity of which is given by Q_s again.

In contrast to the glasma stage, the time scale when the hydrodynamic model starts working is of order $\tau \lesssim 1\ \mathrm{fm}/c$. It is an urgent theoretical problem to fill in the gap between these times scales. Along this line there are many theoretical attempts based on the glasma simulation [5–7], the plasma instability [8], the hard-loop expansion [9], the kinetic description [10], the holographic duals [11,12], and the classical Yang–Mills simulations [13,14].

In this work we solve the Yang–Mills equation of motions starting with the glasma initial condition. The question is then: what is the most likely candidate for the mechanism to "decohere" the longitudinal $\mathcal{E}^\eta$ and $\mathcal{B}^\eta$ on such a short time scale? This kind of decoherence problem is a quite generic problem that we may encounter in various circumstances (see, e.g., Ref. [15] for a scalar-model study). Our proposal is that turbulent diffusion should be the driving force for this; indeed it is known in many physical phenomena that turbulence is a much faster process than the typical molecular diffusion by several orders of magnitude.

In the context of the RHIC and LHC physics, the role of turbulence has been emphasized as a possible account for the smallness of the ratio of viscosity to the entropy density [16]—because energy transport is efficient, an anomalously small viscosity arises generally in a turbulent flow. The actual calculation assumes a random background distribution of chromo fields [17]. Therefore, we still need to consider from where these fields are generated, and the glasma simulation is indispensable to answer such a question. The turbulence, especially the wave turbulence, has also been investigated numerically and analytically [18–21]. It has been understood that the Kolmogorov-type cascade leads to a power-law spectrum (where the power index may take different values at strong coupling). The Kolmogorov behavior is, however, realized in a system with a well-developed inertial region [22]. This means that we have to wait for a certain time until the power-law spectrum grows steadily, while what we want to clarify is not the steadiness but the rapid reorganization from the initial state. We should, therefore, disturb the initial system with substantially large fluctuations that breach the boost invariance.

For this purpose, in this work, we turn off the effect of the expanding geometry. We do this because the expanding geometry is singular at the initial time, and it is difficult to disturb the initial state without ambiguity. Besides, the expansion quickly renders the transverse dynamics frozen, so one should carefully formulate the initial spectral shape (involving the UV divergence) and also elaborate the proper renormalization (or subtraction) procedures [15,23]. Otherwise, useful information on the underlying physics can be easily diluted and even concealed by the effect of expansion. These are not simply technical problems; the expanding geometry represents curved spacetime and quantum fluctuations on such curved spacetime are distorted, so that the physical vacuum should be Bogoliubov transformed from the vacuum in flat spacetime. Interestingly enough, as we will find later, a particular initial condition corresponding to the heavy-ion collision already captures the essential features of the anisotropic dynamics. Moreover, we have checked whether we can confirm the same observation using a code for the expanding case and have

found similar behavior if we employ large fluctuations, while the nonexpanding simulation always leads to inhomogeneous pattern formation for any (small) fluctuations.

One might feel that the approximation of adopting a nonexpanding box is an artificial simplification. However, it is just obvious that the expansion effects should delay the decohering processes, so one must first understand the decohering mechanism for the nonexpanding system; otherwise it is impossible to give any account for the expanding case. Then, one should test the presumed mechanism to see whether it works to overcome the delay in the expanding case. This is why we dare to drop the expansion off; the relevance to the experiment becomes less, but the theory becomes more well behaved thanks to this simplification.

The most important point in this work is that the longitudinal and transverse dynamics behave totally differently at early time when the anisotropy from the collision geometry is huge. One can presume by intuition that the longitudinal decoherence should go much faster than the transverse one; otherwise the isotropization is never achieved. Indeed, we will confirm this anticipation and find that it indeed happens in a very interesting manner.

II. FORMULATION

Most importantly, we can make use of the glasma initial condition [24,25] as it is even in the nonexpanding case because the initial fields lie only in the transverse plane. In terms of the link variables on the lattice, the canonical momenta leads to the following time evolution:

$$U_i(t+2\Delta t) = \exp[-igE^i(t+\Delta t)2\Delta t]U_i(t), \tag{1}$$

where the time arguments are shifted in accord to the leapfrog algorithm which preserves exactly Gauss's law. We omit writing the lattice spacing a throughout this paper. The classical Yang–Mills equations of motion (Hamilton's equations) read

$$E^i(t+\Delta t) - E^i(t-\Delta t) = 2\Delta t \frac{i}{2g}\sum_{j\neq i}[U_{ji}(t) + U_{-ji}(t) - (\text{H.c.})] \tag{2}$$

in the temporal axial gauge; $U_t = 1$. The initial condition is given in a standard way, which simplifies particularly for the SU(2) color group [25] as

$$U_i = \left(U_i^{(1)} + U_i^{(2)}\right)\left(U_i^{(1)\dagger} + U_i^{(2)\dagger}\right)^{-1}, \tag{3}$$

$$E^z = \frac{-i}{4g}\sum_{i=x,y}\left\{(U_i - 1)\left(U_i^{(2)\dagger} + U_i^{(1)\dagger}\right) + [U_i^\dagger(x-\Delta x_i) - 1] \times \left[U_i^{(2)\dagger}(x-\Delta x_i) - U_i^{(1)\dagger}(x-\Delta x_i)\right] - (\text{H.c.})\right\}, \tag{4}$$

with the pure gauge configurations, $U_i^{(m)}(\boldsymbol{x}_\perp) = V^{(m)}(\boldsymbol{x}_\perp)V^{(m)\dagger}(\boldsymbol{x}_\perp + \Delta x_i)$, and the gauge rotation, $V^{(m)\dagger} = e^{ig\Lambda^{(m)}}$, by the static potential obtained as a solution of the Poisson equation, $\partial_\perp^2\Lambda^{(m)} = -\rho^{(m)}$.

We assume the Gaussian distribution for the color source, $\langle\rho^{(n)}(\boldsymbol{x}_\perp)\rho^{(m)}(\boldsymbol{x}'_\perp)\rangle = \delta^{nm}g^2\mu^2\delta(\boldsymbol{x}_\perp - \boldsymbol{x}'_\perp)$, where μ is supposed to be related to the characteristic scale Q_s as was mentioned in the previous section. If we solve the time evolution with the initial conditions (3) and (4), there would appear to be no dependence on the longitudinal coordinate (i.e., z in the present case without expansion, corresponding to η in Bjorken coordinates). This means that QCD color strings extend along the z direction at initial time. We shall introduce a minimal perturbation to make it the clearest how these strings are disrupted by extra fluctuations:

$$E^i = g^3\mu^2[f(z-\Delta z) - f(z)]\xi^i, \quad f(z) = \Delta\cos(2\pi z/L_z), \tag{5}$$

where $\langle\xi^i(\boldsymbol{x}_\perp)\xi^j(\boldsymbol{x}'_\perp)\rangle = \delta^{ij}\delta^{(2)}(\boldsymbol{x}_\perp - \boldsymbol{x}'_\perp)$ and δE^η is solved from Gauss's law. In this way we put a seed of electric-field amplitude $\propto\Delta$ at the lowest nonzero momentum $|k_z^{(\min)}| = 2\pi/L_z$. As long as the instability stays weak, the linear superposition gives a good approximation for the results with more general fluctuations [7]. In this work, however, we will also choose a nonsmall Δ to test the robustness of what we discover. In principle, we should generate quantum fluctuations according to the ground-state (Gaussian) wave function and take the ensemble average over all fluctuations, which would lead to the UV divergence of the zero-point oscillation energy. To avoid this complication, in this work, we pick up a "representative" of the configuration by Eq. (5). This simplification would affect quantitative details such as the precise time scale of the decoherence, but should be harmless to the qualitative nature of the phenomenon that we will discuss.

III. NUMERICAL RESULTS

First let us address the case without z-dependent fluctuations. With unbroken translational invariance in the z direction, the transverse pressure P_T approaches a finite value, while the longitudinal pressure P_L decreases to vanish asymptotically, where they are, respectively, defined as

$$P_\mathrm{L} = \mathrm{tr}[(E^x)^2 + (E^y)^2 - (E^z)^2 + (B^x)^2 + (B^y)^2 - (B^z)^2],$$
$$P_\mathrm{T} = \mathrm{tr}[(E^z)^2 + (B^z)^2]. \tag{6}$$

In our numerical computation we use $g^2\mu = 120/L_\perp$ (corresponding to the choice $g^2\mu \sim 2$ GeV) with $g = 2$ and the transverse and longitudinal site numbers, $L_\perp = L_z = 96$. This is a conventional choice of parameters following Ref. [4], but the classical approach would be more well defined with a smaller g. The most important for the validity of the classical approach is, however, not the choice of g but the scale of the quantities we look at. That is, the classical description should be reasonable for quantities with momentum scale smaller than Q_s. With the above parameters the transverse lattice spacing is of the same order as Q_s^{-1}, so that the classical approach can be legitimate to capture phenomena over several lattice sites, as we will see later.

We note that the initial energy density is both UV and IR singular [26]:

$$\varepsilon(t=0) = N_\mathrm{c}\left(N_\mathrm{c}^2 - 1\right)\frac{(g^2\mu)^4}{8\pi^2 g^2}\left[\ln\frac{\Lambda_\mathrm{UV}}{m_\mathrm{IR}}\right]^2, \tag{7}$$

where Λ_UV and m_IR are UV and IR cutoff scales, respectively. This singularity is problematic in a nonexpanding box, while

the time evolution soon diminishes this singularity in the expanding case [26]. In our numerical simulation, thus, we need to introduce a UV cutoff $(k_\perp)_{\max}$ when we solve the Poisson equation, i.e., higher modes with $k_\perp > (k_\perp)_{\max} = 32 \times 2\pi/L_\perp \sim 1.7 g^2\mu \sim 3.4$ GeV are dropped to get the results presented in this paper. We have then confirmed that our results have only minor dependence on $L_\perp$ as long as we keep the same $(k_\perp)_{\max}$. We also note that, because of the color string, the initial P_L starts from a negative value (i.e., two nuclei feel an attractive force).

It is already a nontrivial observation that P_L vanishes at late time. In the expanding case, since the system is stretched and diluted, one may anticipate $P_L \to 0$ as a result of the free streaming. In the present simulation, however, the box does not expand and nothing streams out, so that $P_L \to 0$ is purely realized by the choice of the initial conditions (3) and (4). This implies that $P_L \to 0$ even in the expanding glasma should be attributed not to the expansion but to the initial conditions. In other words, the free streaming is not the reason, but the physical interpretation of the result.

We shall next proceed to the results with z-disturbing fluctuations, as shown in Fig. 1. We here adopt three different Δ; a substantially large $\Delta = 0.2$ gives the energy density from fluctuations of the same order of magnitude as the background fields. Therefore, this value is a kind of upper bound above which solving the classical equations of motion is no longer justified. A marginal $\Delta = 0.02$ is much safer; the initial energy density is dominated by the background fields, and the time evolution is almost identical to the case with even smaller $\Delta = 0.002$, as is manifested in Fig. 1. (To avoid making the figure too busy, we did not show the fluctuation-free results with $\Delta = 0$ that behave like the results with $\Delta = 0.02$ or 0.002 till $g^2\mu t \sim 60$ and monotonically approach zero beyond it.)

There are two interesting observations that one can notice at a glance. First, the choices of $\Delta = 0.02$ and 0.002 make only little change in the onset of the instability around $g^2\mu t \sim 100$ where P_L/P_T start growing. Owing to this, we can be very sure that our results should be robust at least on a qualitative level regardless of our ignorance of the precise value of Δ. We note that, as long as the amplitude of each unstable mode is small in the linear regime, it should obey a simple scaling law of proportionality with Δ as observed in Ref. [7], while the time evolution is fixed by the background fields and is rather insensitive to Δ. Because Fig. 1 shows not a mode amplitude but a bulk pressure involving all modes, it is not transparent how the results exhibit the scaling law with Δ. Nevertheless, the similar behavior with $\Delta = 0.02$ and 0.002 suggests that the onset time is predominantly determined by the properties of the background fields unless large fluctuations could affect the background fields.

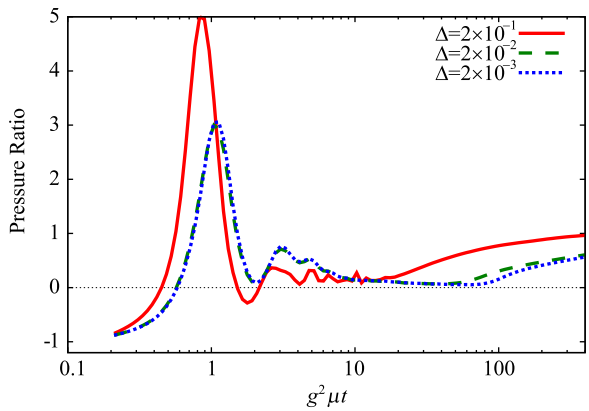

FIG. 1. (Color online) Pressure ratio P_L/P_T as a function of dimensionless time. Without fluctuation the ratio approaches zero, while it goes to a nonzero constant if fluctuations are implemented. An ensemble average is taken over 50 configurations.

Second, if Δ is less than $\sim$0.2, we cannot reach the complete isotropization. (In principle, if we wait forever, it may achieve complete isotropization, though we could not confirm it in our long-time simulation.) This is quite unexpected: Because the simulation runs in the isotropic setup, the anisotropy given at the initial time should naturally fade out if we wait for a sufficiently long time. This intuition is correct, but the point is that it takes an extraordinarily long time unless Δ is so large that it also modifies the initial energy density. It is quite instructive to see that *the isotropization at later time is a very slow process* even in a nonexpanding and symmetric box. Here we make a comment on recent results in Ref. [27] where a tendency toward isotropization was observed. Our claim is consistent with their finding: *complete* isotropization ($P_L = P_T$) is difficult to realize but 50%–60% of isotropization would be more realistic, as seen in Ref. [27] and in this present study.

To discuss more microscopic dynamics, we shall split the time evolution into three distinct characteristic regimes as shown below.

A. Temporarily and spatially oscillatory regime

The pressure has oscillatory behavior in the earliest stage (i.e., $g^2\mu t \lesssim 15$ for $\Delta = 0.2$ and $g^2\mu t \lesssim 50$ for $\Delta = 0.02$ as deduced from Fig. 1). The so-called glasma instability must be developing from lower to higher longitudinal modes, but their effects are not yet appreciable in the bulk thermodynamics at zero mode. In the phenomenological sense, the theoretical understanding in this regime is the most crucial issue, while many theoretical efforts had been devoted to rather later-time dynamics. Hence, our central objective in this present paper is to shed light on this oscillatory regime.

Obviously, the equation of state still has fast components in time, which means that the derivative expansion should not work. One cannot therefore apply the hydrodynamic equations to describe the time evolution yet. Then, a natural question arises; what about the spatial structure? Is it already smooth enough or linked somehow to the rough structure in time?

To diagnose the microscopic dynamics, we make three-dimensional (3D) and density plots to illustrate the cascade flow of the energy spectrum toward higher k_z or the wave number n_z (where $k_z = n_z 2\pi/L_z$) in the longitudinal direction. We define the following energy spectrum with only the z direction Fourier transformed as

$$\varepsilon(x,y,k_z) = \sum_i \mathrm{tr}[E^i(x,y,-k_z)E^i(x,y,k_z) + B^i(x,y,-k_z)B^i(x,y,k_z)], \quad (8)$$

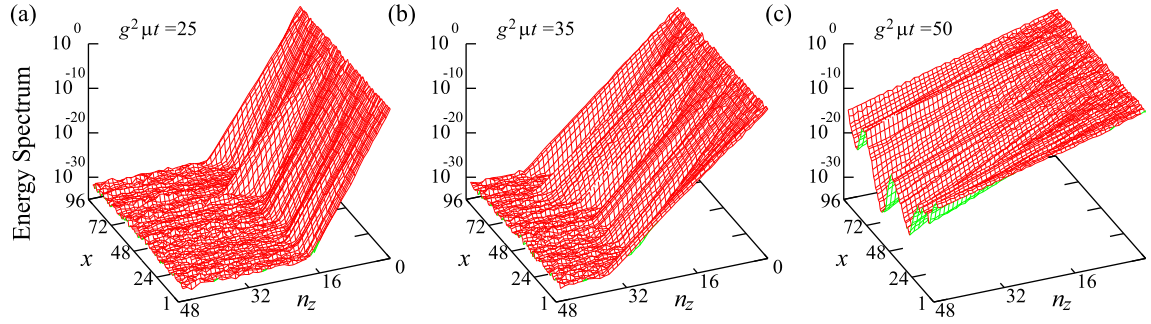

FIG. 2. (Color online) Energy spectrum as a function of the coordinate x (in unit of a) and the momentum k_z with $y = L_y/2$ fixed, calculated for $\Delta = 0.02$. The far left (a) represents the result at the initial time $g^2\mu t = 0.2$, and the time increments up to $g^2\mu t = 50$ of (c) at the right.

which is measured for each configuration. This is not a gauge-invariant quantity and we need to fix the gauge to *define* it uniquely. We already chose the temporal axial gauge but time-independent gauge rotations are still redundant, which does not change the gauge-invariant observable but modifies $\varepsilon(x,y,k_z)$. Therefore, we fix the initial gauge configurations (3) and (4) (with fluctuations included) to satisfy the Coulomb-gauge condition $\boldsymbol{\nabla}\cdot\boldsymbol{A} = 0$ that would flatten spiky textures. We used the over-relaxation method with 1000 steps to impose the Coulomb gauge and explicitly checked that the gauge configurations become extremely smooth then.

For qualitative discussions we may choose any Δ, in principle, but to remove an impression that our findings come from artificially large Δ, we here adopt a rather safer choice of $\Delta = 0.02$ that has no effect on the very early dynamics as is clear from Fig. 1. Then, for graphical purpose, we pick a slice of $y = L_y/2$ up and make a 3D plot of $\varepsilon(x,y,k_z)$ as a function of x and n_z in Fig. 2 for *one* configuration.

We can understand from Fig. 2 what is actually happening on the microscopic level during the oscillatory regime. In this very first stage the energy amplitude spreads toward larger k_z triggered by spots localized in x (and y) space. These localized spots look like narrow avalanches. Let us here "define" what we really mean by *avalanche* for clarity.

To do so, we have to magnify the initial energy stored at $n_z = 0$ mode, which is presented in Fig. 3. It should be noted that this is nothing but the energy distribution already shown in Fig. 2(a) in the form of a logarithmic plot. Even though Fig. 3 may look like it has a rough structure, the energy fluctuates within only one order of magnitude. It is evident from Figs. 2(b) and 2(c) that the inhomogeneity developing later at larger n_z is correlated to the initial pattern, and the resulting intensity differs by more than ten orders of magnitude! We would call this huge (but relative) amplification of the spatial pattern the *avalanche* phenomenon.

This type of the avalanche phenomenon is quite common in many physics problems. The avalanche breakdown of an insulator or semiconductor is one familiar example in which free electrons trigger the creation of electron-hole pairs. In the present glasma simulation, we have specified both the initial conditions (3) and (4), and the initial fluctuations (5) according to the Gaussian distribution, and some local positions happen to have irregular amplitudes as observed in Fig. 3, which is responsible for the avalanches. Probably they have much to do with the magnetic vortices discovered recently in the same model setup [28]. We here point out that these narrow avalanches are collective consequences from the simultaneous existence of the glasma fields and the fluctuation fields. We turned the glasma background fields off as a test calculation, and we found that the amplitudes just smoothly and slowly decayed into higher k_z, but no rapid narrow avalanche emerged.

These avalanche-like structures gradually spread over x (and y) space as time elapses, and eventually the distribution appears uniform in transverse space at a further later time, which we call *transverse diffusion*. To access the full transverse structure and visualize the diffusion, we show $\varepsilon(x,y,k_z)$ as snapshots in Fig. 4 at $g^2\mu t = 35$, 50, and $g^2\mu t = 75$ using the same configuration as was used to draw Fig. 2. We can then clearly perceive the dynamical pattern formation in the transverse geometry and subsequent diffusion; at localized spots with brighter colors we have larger amplitudes for the maximum k_z mode, namely, $k_z^{(\max)} = (L_z/2)(2\pi/L_z) = \pi/2$ (in units of a^{-1}). To the best of our knowledge the present analysis is the very first demonstration that has revealed the spontaneous generation of spatial patterns in a real-time simulation of the Yang–Mills theory. At the same time as we emphasize the novelty, we would also like to draw attention to the similarity to many other systems out of equilibrium: One intuitive example lies in the formation of the magnetized

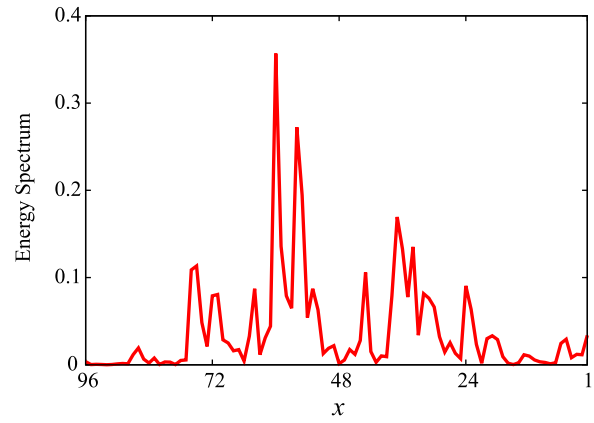

FIG. 3. (Color online) Energy spectrum corresponding to Fig. 2 for $\Delta = 0.02$ at $n_z = 0$ at the initial time $g^2\mu t = 0.2$ and shown on a linear scale.

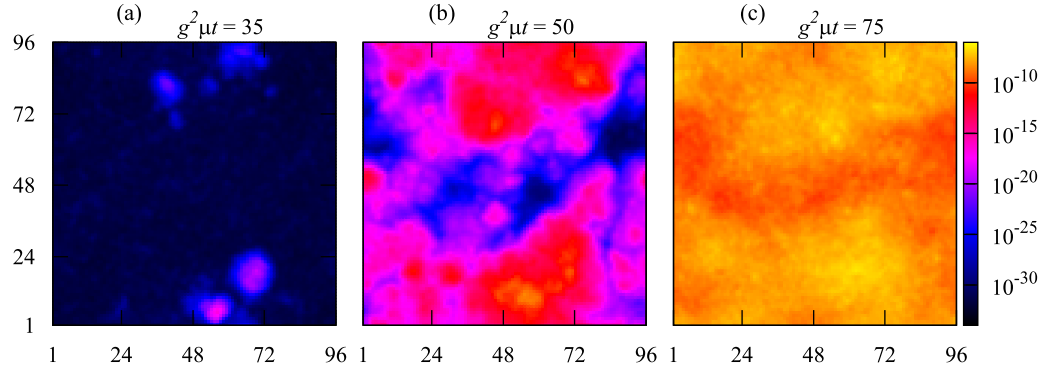

FIG. 4. (Color online) Snapshots of the energy amplitude for $\Delta = 0.02$ at maximum k_z on the transverse x-y plane (in units of a). These are taken at the times corresponding to Fig. 2. Clearly a dynamical pattern is formed first and the region with high k_z next spreads over the transverse directions.

domains described by the time-dependent Ginzburg–Landau theory of the classical spin models. Such a pattern was numerically discovered in the direction from the random initial state to the ordered spin state at lower T, and amazingly also in the opposite direction from the enforced ordered (or coherent) state to the disordered (or decoherent) spin state at high T [29]. Our results are reminiscent of the latter associated with nonequilibrium decohering processes.

Let us quantify the transverse diffusion processes by calculating the energy-density correlation function from Fig. 4 or the "power spectrum" defined by

$$P(k_\perp) = \left\langle \varepsilon\left(-k_\perp, k_z^{(\max)}\right)\varepsilon\left(k_\perp, k_z^{(\max)}\right)\right\rangle, \tag{9}$$

where we note that the meaning of $k_\perp$ is totally different from k_z; we introduced $k_\perp$ as the Fourier transform of x and y of $\varepsilon(x,y,k_z)$, while k_z refers to the momentum carried by the chromo-electric and chromo-magnetic fields.

To absorb orders-of-magnitude differences at different times, we normalize the power spectrum by the zero-mode value $P(0)$ and draw Fig. 5 for $g^2\mu t = 25$, 50, and 75.

We can clearly confirm that the long-range correlation becomes more and more enhanced as time goes on, which is quite consistent with what we can see from Fig. 4. (We note that the wave number, say 10 on this plot, corresponds to the physical scale, $10 \times 2\pi/L_\perp \sim 1$ GeV.) The reason why the normalized power spectrum seemingly looks more suppressed at larger $g^2\mu t$ is that the zero-mode grows larger. Thus the relative height decreases, although the absolute height is much larger at later time. It should be clearly noted here that we should *not* take this enhancement of the long-range correlation for a signal of the Bose-Einstein condensate, as speculated in Ref. [30]. We are now looking not at the particle distribution but at the energy-density correlation. We observe that the spots in the transverse plane spread out quickly toward uniformity, which is to be interpreted as the diffusion as can be inferred from Fig. 4.

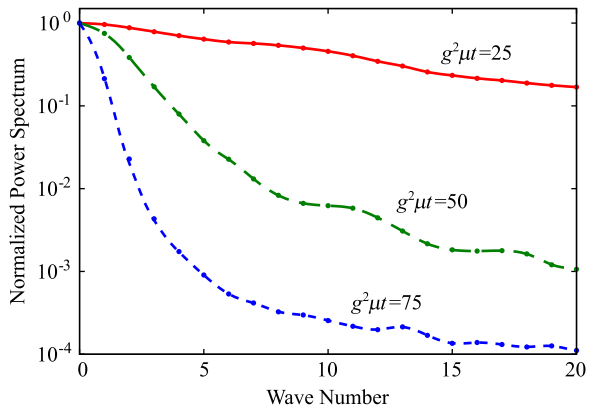

FIG. 5. (Color online) Power spectrum $P(k_\perp)$ as a function of transverse wave number, normalized by the zero-mode value. The ensemble average is taken over 50 configurations.

B. Intermediate fast-growing regime

After some time ($15 \lesssim g^2\mu t \lesssim 30$ for $\Delta = 0.2$ and $50 \lesssim g^2\mu t \lesssim 100$ for $\Delta = 0.02$ in Fig. 1) the equation of state behaves smoothly enough in time and also in space, which should enable the hydrodynamic evolution to work fine during this regime since the derivative expansion makes sense. The system still goes on approaching isotropization, and thus it is neither isotropic nor thermalized yet. An important question is what determines the typical time scale for the transition from the oscillatory regime to the growing regime. In other words, we need to know what is still missing to accelerate the onset time for the hydrodynamic evolution. The time scale is characterized by the balance between the initial energy density stored at the zero mode and the rate of the energy flow that is intrinsically determined by the Yang–Mills interactions. Within the present framework it is difficult to yield the onset time around a few times $g^2\mu \sim 2$ GeV ~ 0.1 fm/c as required by the analysis of the experimental data.

It is important not to be confused by the behavior of the most unstable mode in the expanding case [5,7], which looks very similar to Fig. 1. In the expanding case the onset is delayed simply by the kinematical reason [6], and in the nonexpanding case in Fig. 1 it is not the most unstable component but the whole pressure that we are dealing with. Therefore it takes time for the instability to spread over the whole phase space.

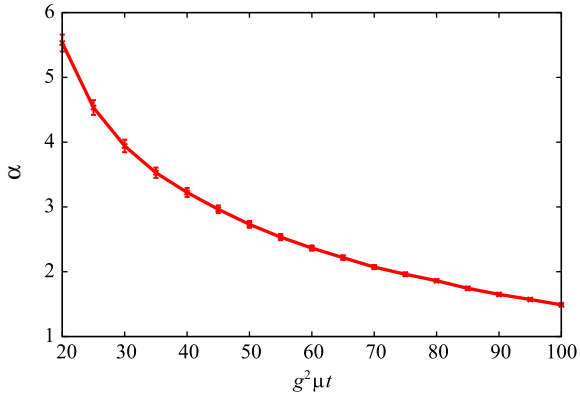

FIG. 6. (Color online) Power index deduced from the tail of the energy spectrum fit by $k_z^{-\alpha}$ given as a function of dimensionless time.

C. Asymptotic slowly growing regime

The diffusion is caused by inhomogeneity, and so it becomes slower and slower with less and less inhomogeneity and anisotropy. Naturally the tendency toward isotropization becomes weakened as $P_{\rm L}$ and $P_{\rm T}$ get closer to each other. In such an asymptotic regime ($g^2\mu t \gtrsim 30$ for $\Delta = 0.2$ and $g^2\mu t \gtrsim 100$ for $\Delta = 0.02$ in Fig. 1) the characteristic time scale, if taken literally, seems to be too long as compared to the typical time scale in the experiment. If we take a smaller g and thus larger Q_s, however, hundreds of Q_s would still be within a reasonable time window that is relevant to the thermalization process in the heavy-ion collision.

Usually some kind of scaling law may be observed in a well-developed turbulent system at late time. In the present simulation with specific initial conditions (3) and (4), however, the zero mode cannot be a consistent source to supply the energy injection and so it cannot sustain a steady inertial region in the energy spectrum. Still, there may be a chance to see scaling behavior at the tail of the energy spectrum. To test this idea, we attempt to fit the longitudinal energy spectrum by the power-law spectrum $\sim k_z^{-\alpha}$, and we find that the fit works well in the range, $n_z = 25 \sim 48$. Then, the power α turns out to be a function of time as in Ref. [19], which is plotted in Fig. 6. The value of the index α decreases with increasing time, which crosses the Kolmogorov value $5/3 = 1.67$ and becomes even smaller. As we discussed above, the inertial region is not stable and the precise value of α is not very important in the present case but this level of qualitative agreement is quite suggestive. One might care about the consistency with Ref. [18] in which a stable power law has been identified. We note that this difference between the present analysis and Ref. [18] comes from the totally different choice of initial conditions (3) and (4) that resemble the anisotropy in a heavy-ion collision.

IV. CONCLUSIONS

With the results from our numerical simulations, we arrive at the picture of the very-early-time stage in a relativistic heavy-ion collision sketched in the illustration of Fig. 7.

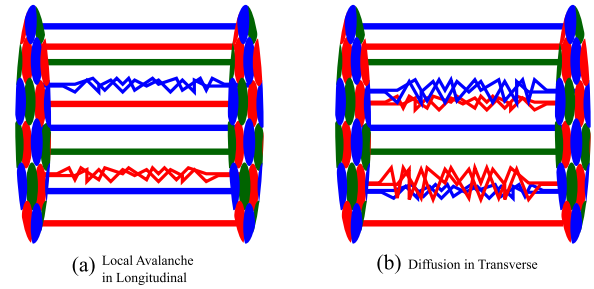

FIG. 7. (Color online) Schematic picture of two fastest processes in the early-time dynamics in a relativistic heavy-ion collision.

The fastest process is driven by the avalanche-like decay along the longitudinal direction which takes place locally in the transverse plane. These avalanches are to be attributed to initial fluctuations. Once this occurs, the boost invariance or the z invariance is quickly but only locally broken as in Fig. 7(a). This view also invokes the famous Reynolds' experiment of turbulent flow inside a pipe [31] where the translationally steady flow of ink begins wandering under disturbances if the Reynolds' number exceeds a critical point. From this analogy it may well be reasonable to identify these local avalanches as the appearance of a sort of fluid turbulence. Also, it would be conceivable to associate them with the QCD string breaking which is accompanied by the particle production.

The next vital fast process is the diffusion over the transverse plane. This turbulent diffusion is quite an efficient mechanism to dispose of energy in the whole phase space, and eventually to let the equation of state behave smoothly enough.

Before addressing the possible relevance to the experimental data, the following upgrades should be taken into account: First, it is necessary to incorporate the full quantum spectrum that should further accelerate the process speed. Second, related to this, we should carefully deal with the renormalization and subtract the UV divergence originating from the quantum fluctuation. Third, we need to turn the expansion on, which makes it even more subtle to handle the first and the second points above. In principle, as we commented, the avalanches should be associated with the particle production, which is to be reflected in the moments of the angular distribution of the produced particles. For quantitative theoretical prediction, however, we must tackle the tough above-mentioned obstacles and complete the thermalization scenario first. We believe that the qualitative finding reported in this work should be a crucial step toward solving the puzzle of the thermalization problem.

ACKNOWLEDGMENTS

K.F. thanks Guy Moore for comments on gauge fixing, Thomas Epelbaum for useful communications, and Maximilian Attems, Francois Gelis, Yoshimasa Hidaka, and Keiji Saito for discussions. He was supported by JSPS KAKENHI Grant No. 24740169.

[1] For a review on the finite-T lattice simulation, see O. Philipsen, Prog. Part. Nucl. Phys. **70**, 55 (2013).

[2] For a review on the hydrodynamic models, see T. Hirano, P. Huovinen, K. Murase, and Y. Nara, Prog. Part. Nucl. Phys. **70**, 108 (2013).

[3] For reviews on the saturation effect in high-energy QCD, see E. Iancu, A. Leonidov, and L. McLerran, arXiv:hep-ph/0202270; E. Iancu and R. Venugopalan, in *Quark Gluon Plasma*, edited by R. C. Hwa *et al*., arXiv:hep-ph/0303204; L. McLerran, Acta Phys. Pol. B **41**, 2799 (2010) [arXiv:1011.3203 [hep-ph]].

[4] T. Lappi and L. McLerran, Nucl. Phys. A **772**, 200 (2006).

[5] P. Romatschke and R. Venugopalan, Phys. Rev. Lett. **96**, 062302 (2006); Phys. Rev. D **74**, 045011 (2006).

[6] H. Fujii and K. Itakura, Nucl. Phys. A **809**, 88 (2008); H. Fujii, K. Itakura, and A. Iwazaki, *ibid*. **828**, 178 (2009).

[7] K. Fukushima and F. Gelis, Nucl. Phys. A **874**, 108 (2012).

[8] S. Mrowczynski, Phys. Lett. B **314**, 118 (1993); Acta Phys. Pol. B **37**, 427 (2006) [arXiv:hep-ph/0511052].

[9] S. Mrowczynski, A. Rebhan, and M. Strickland, Phys. Rev. D **70**, 025004 (2004); A. Rebhan, P. Romatschke, and M. Strickland, Phys. Rev. Lett. **94**, 102303 (2005); J. High Energy Phys. 09(2005)041; A. Rebhan, M. Strickland, and M. Attems, Phys. Rev. D **78**, 045023 (2008); M. Attems, A. Rebhan, and M. Strickland, *ibid*. **87**, 025010 (2013).

[10] E. L. Bratkovskaya, W. Cassing, C. Greiner, M. Effenberger, U. Mosel, and A. Sibirtsev, Nucl. Phys. A **675**, 661 (2000); V. Ozvenchuk, E. Bratkovskaya, O. Linnyk, M. Gorenstein, and W. Cassing, EPJ Web Conf. **13**, 06006 (2011); M. Ruggieri, F. Scardina, S. Plumari, and V. Greco, arXiv:1303.3178.

[11] R. A. Janik and R. B. Peschanski, Phys. Rev. D **74**, 046007 (2006); M. P. Heller and R. A. Janik, *ibid*. **76**, 025027 (2007); M. P. Heller, R. A. Janik, and P. Witaszczyk, Phys. Rev. Lett. **108**, 201602 (2012).

[12] P. M. Chesler and L. G. Yaffe, Phys. Rev. Lett. **102**, 211601 (2009); Phys. Rev. D **82**, 026006 (2010); V. Balasubramanian, A. Bernamonti, J. de Boer, N. Copland, B. Craps, E. Keski-Vakkuri, B. Müller, A. Schäfer *et al*., Phys. Rev. Lett. **106**, 191601 (2011); Phys. Rev. D **84**, 026010 (2011); M. P. Heller, D. Mateos, W. van der Schee, and D. Trancanelli, Phys. Rev. Lett. **108**, 191601 (2012).

[13] B. Muller and A. Trayanov, Phys. Rev. Lett. **68**, 3387 (1992); T. S. Biro, C. Gong, B. Muller, and A. Trayanov, Int. J. Mod. Phys. C **5**, 113 (1994); G. D. Moore, Nucl. Phys. B **480**, 689 (1996); C. R. Hu and B. Muller, Phys. Lett. B **409**, 377 (1997); T. Kunihiro, B. Muller, A. Ohnishi, A. Schafer, T. T. Takahashi, and A. Yamamoto, Phys. Rev. D **82**, 114015 (2010); H. Iida, T. Kunihiro, B. Mueller, A. Ohnishi, A. Schaefer, and T. T. Takahashi, *ibid*. **88**, 094006 (2013).

[14] J. Berges, S. Scheffler, and D. Sexty, Phys. Rev. D **77**, 034504 (2008); J. Berges, S. Scheffler, S. Schlichting, and D. Sexty, *ibid*. **85**, 034507 (2012); J. Berges, K. Boguslavski, and S. Schlichting, *ibid*. **85**, 076005 (2012); J. Berges, S. Schlichting, and D. Sexty, *ibid*. **86**, 074006 (2012).

[15] K. Dusling, T. Epelbaum, F. Gelis, and R. Venugopalan, Nucl. Phys. A **850**, 69 (2011); T. Epelbaum and F. Gelis, *ibid*. **872**, 210 (2011).

[16] M. Asakawa, S. A. Bass, and B. Muller, Phys. Rev. Lett. **96**, 252301 (2006); Prog. Theor. Phys. **116**, 725 (2007).

[17] M. Kirakosyan, A. Leonidov, and B. Muller, Acta Phys. Pol. B Proc. Suppl. **6**, 403 (2013).

[18] J. Berges, S. Scheffler, and D. Sexty, Phys. Lett. B **681**, 362 (2009); M. E. Carrington and A. Rebhan, Eur. Phys. J. C **71**, 1787 (2011).

[19] S. Schlichting, Phys. Rev. D **86**, 065008 (2012).

[20] A. Kurkela and G. D. Moore, Phys. Rev. D **86**, 056008 (2012).

[21] J. Berges, K. Boguslavski, S. Schlichting, and R. Venugopalan, arXiv:1303.5650.

[22] V. E. Zakharov, V. S. L'Vov, and G. Falkovich, *Kolmogorov Spectra of Turbulence I: Wave Turbulence* (Springer, Berlin, 1992).

[23] K. Fukushima, F. Gelis, and L. McLerran, Nucl. Phys. A **786**, 107 (2007); K. Dusling, F. Gelis, and R. Venugopalan, *ibid*. **872**, 161 (2011).

[24] A. Kovner, L. D. McLerran, and H. Weigert, Phys. Rev. D **52**, 6231 (1995).

[25] A. Krasnitz and R. Venugopalan, Nucl. Phys. B **557**, 237 (1999).

[26] Y. V. Kovchegov, Nucl. Phys. A **762**, 298 (2005); T. Lappi, Phys. Lett. B **643**, 11 (2006); K. Fukushima, Phys. Rev. C **76**, 021902(R) (2007); **77**, 029901(E) (2008); H. Fujii, K. Fukushima, and Y. Hidaka, *ibid*. **79**, 024909 (2009).

[27] T. Epelbaum and F. Gelis, Phys. Rev. Lett. **111**, 232301 (2013).

[28] A. Dumitru, Y. Nara, and E. Petreska, Phys. Rev. D **88**, 054016 (2013); A. Dumitru, H. Fujii, and Y. Nara, *ibid*. **88**, 031503(R) (2013); T. Gasenzer, L. McLerran, J. M. Pawlowski, and D. Sexty, arXiv:1307.5301.

[29] K. Kudo, M. Mino, and K. Nakamura, J. Phys. Soc. Jpn. **76**, 013002 (2007).

[30] J.-P. Blaizot, F. Gelis, J.-F. Liao, L. McLerran, and R. Venugopalan, Nucl. Phys. A **873**, 68 (2012).

[31] K. Avila, D. Moxey, A. de Lozar, M. Avila, D. Barkley, and B. Hof, Science **333**, 192 (2011).